Photoresist flow simulation using the viscous flow model

Won-Young Chung, Tai-Kyung Kim, Young-Tae Kim, [1]Byung-Joon Hwang, Young-Kwan Park, and Jeong-Taek Kong
CAE Team, [1]Advanced technology development Team, Semiconductor R&D Center,
Samsung Electronics Co., Ltd.
San #24, Nongseo-Ri, Giheung-Eup, Yongin-City, Gyunggi-Do, 449-711, Korea
e-mail : wychung@samsung.com

***Abstract*— The PR(photoresist) flow process applied to the contact patterning is difficult to predict and optimize because the process model does not exist. In this paper, the PR flow simulation method using the viscous flow model is developed and applied to examine the effect of initial shape and process conditions on the PR flow phenomena. In addition, this model is used to optimize the layout with the various contacts in the real pattern. This PR flow model linking to lithography and etch ones can predict and optimize the contact patterning process in cell, periphery, and TEG(Test Element Group) areas and analyze defects considering the pre-/post-processes systematically.**

Keywords-component; PR flow; simulation; viscous flow model; layout

I. INTRODUCTION

As the design rule decreases rapidly, the PR flow process becomes necessary for patterning of sub-200nm contact hole. Thus, the contact patterning process is composed of lithography, PR flow, and etch processes. The lithography process is simulated by Solid-C[1] or Prolith[2] and etch results can be obtained by simulation tools[3,4] including PIE[5], the in-house topography simulator. However, the simulation environment of the total contact processes is incomplete due to the absence of the PR flow model.

Because the PR flow process is affected by many parameters such as, contact size, bulk density, flow and photo process condition[6], it is difficult to predict the results and the process optimization is only done by trial-and-errors. Therefore, modeling and simulation of the PR flow process are needed to predict the flow amount for asymmetric contact patterns.

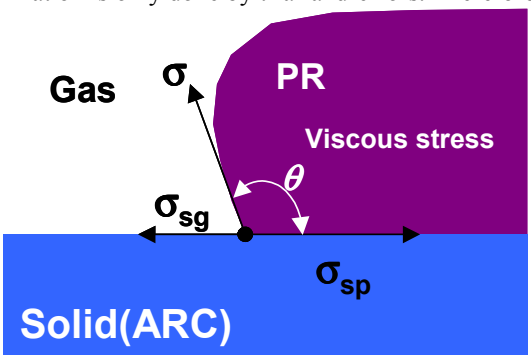

Figure 1. The schematic of the PR flow model (σ: surface tension, θ: contact angle, subscript s: solid, g: gas, p: PR).

In this study, the viscous flow model by the surface tension for the PR flow process and the 3-D transient simulation method are developed and verified for several different PRs. The effects of the key parameters such as the contact size, surrounding bulk density, and temperature on the PR flow are studied through this simulation method. Based on our new methodology, the optimal flow condition of the real patterning process is obtained.

II. RESULTS AND DISCUSSION

A. Modeling of the PR flow

The phenomena of the PR flow were first numerically modeled for process simulation. PR was assumed as fluid which has the viscosity as a function of temperature over Tg(glass transition temperature). As shown in Fig. 1, the surface tension force acts on the interface and then PR flows viscously. The tangential force due to surface tension is expressed as the following Young-Laplace equation :

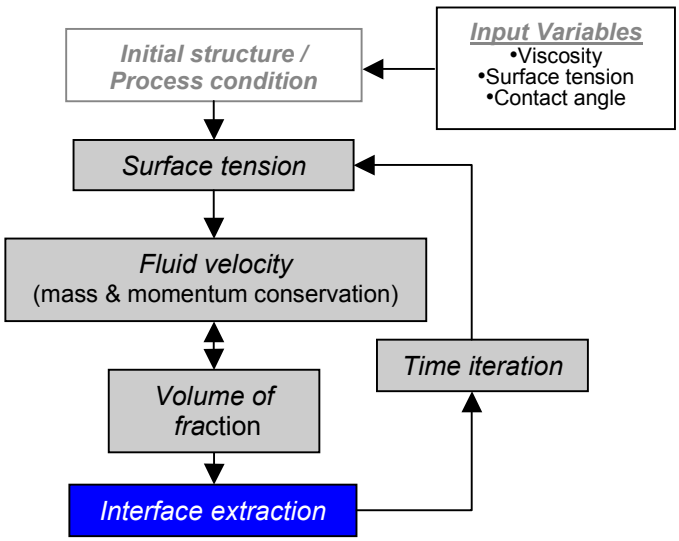

Figure 2. The simulation of the PR flow process

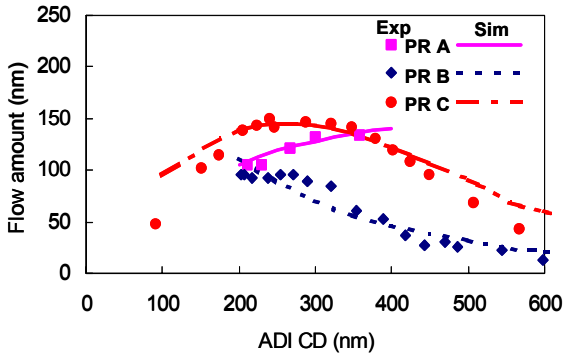

Figure 3. Comparison of simulated and experimental results for different PRs and initial CDs.

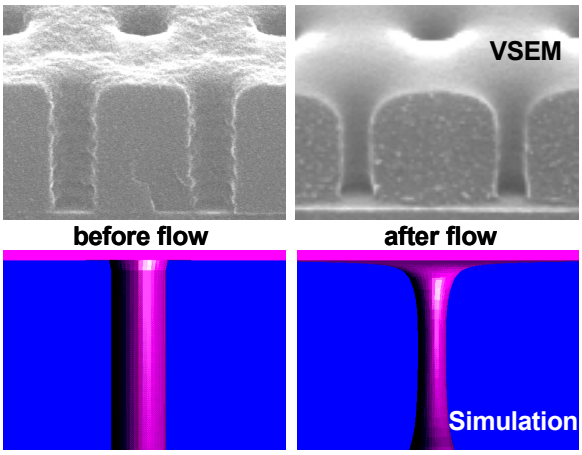

Figure 4. Comparison of vertical profiles of simulation results and VSEMs.

$$\int \Delta p \, ds = \int \tau |d\vec{x}|, \quad \tau = \sigma \vec{n} \times \frac{d\vec{x}}{|d\vec{x}|} \tag{1}$$

where Δp is the pressure difference, σ is the surface tension, $\vec{n}$ is the normal vector of the interface, and $\vec{x}$ is the position vector. The surface tension forces are in equilibrium on the triple interface contacting the substrate by the Young's equation[7], which is given by :

$$\sigma \cos\theta = \sigma_{sg} - \sigma_{sp} \tag{2}$$

where θ is the contact angle and subscript s, g and p mean solid, gas and PR, respectively. The PR moves by these forces. The continuity and Navier-Stokes equations[8] are solved with the following equation:

$$\partial F/\partial t + \nabla \cdot \vec{v} F = 0 \tag{3}$$

where F is the volume fraction of PR, t is the time, and $\vec{v}$ is the velocity vector. The interface between PR and gas is extracted using the volume fraction in each cell and this procedure is iterated during the process time. The simulation procedure of the PR flow process is shown in Fig. 2.

CFD-ACE+[9] was adapted to simulate the PR flow process using this viscous flow model. In addition, the simulation interface by which the result of Solid-C, the lithography simulator, was transferred to initial geometry was set up and the simulation for various contact types and positions became possible from the layout design.

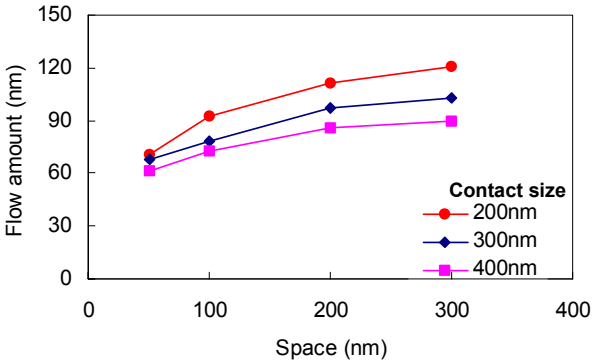

Figure 5. The effect of bulk density on the flow amount for different contact sizes.

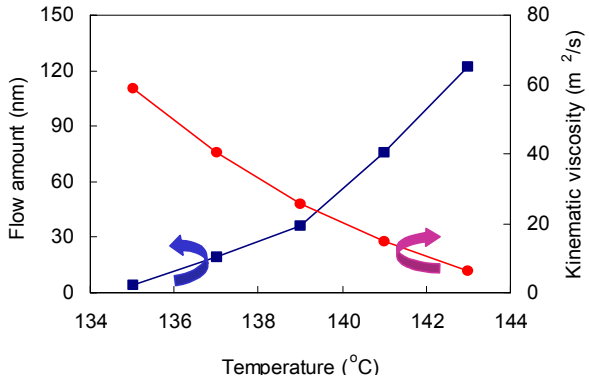

Figure 6. Measured flow amount and extracted viscosity in terms of process temperature.

B. *Validation of model*

Our model and simulation method are evaluated for three different PRs varying the contact diameter as shown in Fig. 3. It shows the different PR flow trends with respect to an initial contact size. The measured amount of the flow for different PRs is well explained by our new model. The vertical profile after the PR flow process became round, which was nearly identical with the simulation result, as shown in Fig. 4.

C. *Effects of initial geometry*

To investigate the effect of the initial PR structure after development on the flow amount, simulations were performed for various initial contact sizes and spaces between contacts. The results for contact sizes are mentioned above and the simulated results for bulk densities are shown in Fig. 5. As the space increased, the flow amount increased proportionally and saturated. It is also known that the bulk density affected the flow amount more for a smaller contact size.

D. *Effects of process temperature*

0-7803-7826-1/03/$17.00 © 2003 IEEE

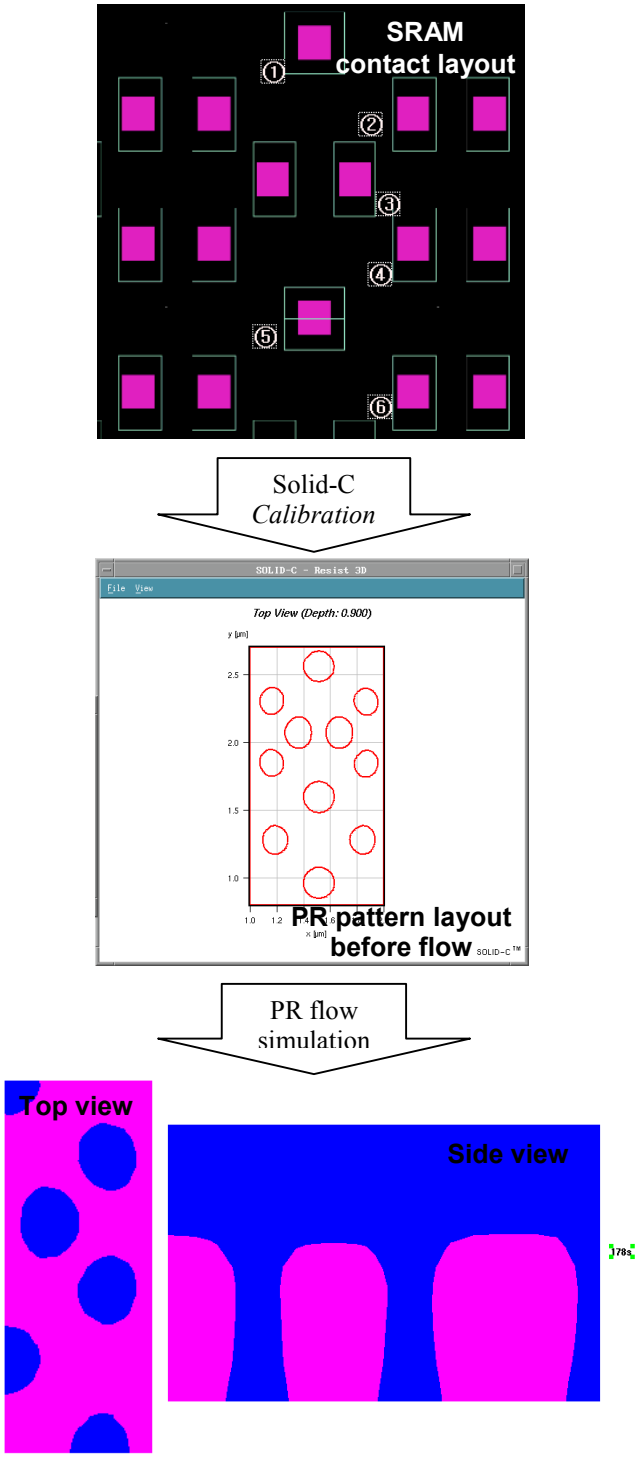

Figure 7. Integration scheme of PR flow with lithography simulation

The PR flow process is generally controlled by adjusting the process time and temperature that change the PR characteristics such as viscosity and surface tension. The PR flow process for a change of temperature can be predicted by calibration of the PR viscosity. Fig. 6 shows the flow amount by the experiments obtained varying the process temperature and the extracted viscosity.

TABLE I. COMPARISON OF SIMULATION RESULTS WITH MEASUREMENTS

Contact type		Simulation	Experiment	Error(%)
Before flow CD (nm)				
1	X	236.0	236.0	0%
2		198.4	208.0	-5%
3		198.6	209.0	-5%
4		200.8	210.0	-4%
5		242.3	243.0	0%
6		205.0	207.0	-1%
1	Y	232.0	223.0	4%
2		231.2	238.0	-3%
3		239.5	257.0	-7%
4		235.4	236.0	0%
5		236.0	228.0	4%
6		266.0	248.0	7%
After flow CD (nm)				
1	X	143.2	147.0	-3%
2		123.3	139.0	-11%
3		127.0	146.0	-13%
4		127.2	140.0	-9%
5		139.4	147.0	-5%
6		116.0	131.0	-11%
1	Y	151.2	136.0	11%
2		132.6	123.0	8%
3		140.6	139.0	1%
4		135.6	117.0	16%
5		143.9	133.0	8%
6		130.8	134.0	-2%

E. Layout and process optimizations

1) Integration scheme with lithography simulation

In the real patterns, the x-, and y-axis CDs of each contact are different and bulk amounts near the contacts also differ, so it is difficult to predict the flow amount and obtain the target CDs. In order to consider the layout effect, the PR flow simulation was integrated with Solid-C, lithography simulation tool, as shown in Fig. 7. First, PR patterns after the photo process are calibrated as input with the layout file. This result is converted as an initial geometry and then PR flow simulation is performed. The last figures of the Fig. 7 show the top and side view after the PR flow.

This integration scheme was applied for the SRAM cell pattern in Fig. 7 and its results are shown in Table I. The simulation reproduced the experimental results in the range of about 15% errors and the order of the contact size became different after the PR flow process, which was also reproduced by the simulation. For example, y-axis CD of contact "1" was less that that of contact "4" before flow, but after flow it became reverse, i.e., the flow simulation showed the same results.

2) Real pattern optimization

The PR flow model integrated with lithography simulation was used to optimize the layout as well as the process condition of the contact patterns of the low power SRAM with 0.1μm design rule. The optimal layout design to get the uniform target contact size was difficult because the array of contact patterns is not orderly and symmetric. Layout modification and process optimization were conducted simultaneously by using the PR flow and lithography simulation. As a result, the

0-7803-7826-1/03/$17.00 © 2003 IEEE

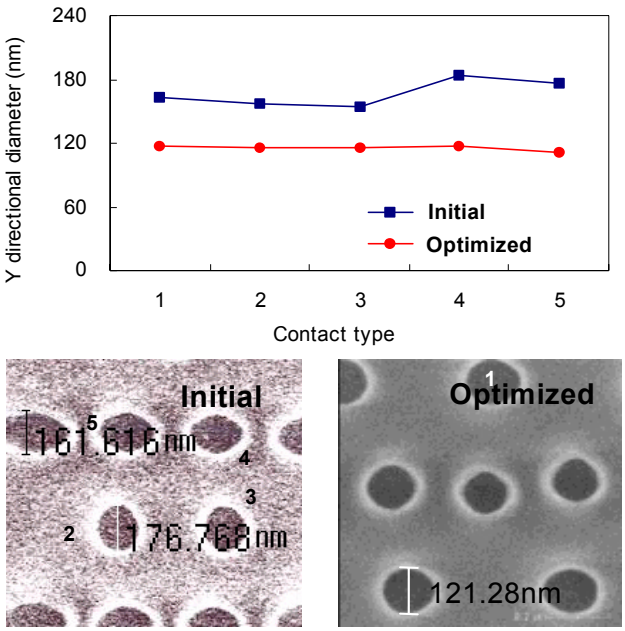

Figure 8. Comparison of simulated contact diameters(graph) and in-line SEMs between before and after optimization.

contact pattern which had the uniform target diameter (~120nm) and the circular shape is obtained, as shown in Fig. 8.

III. CONCLUSIONS

We have developed a new viscous flow model and 3-D transient simulation procedure for the PR flow process that is necessary in contact patterning. We have verified the predictability of this model by comparing with the experimental results. Simulated results for different kinds of PR showed the same trend with the experimental data in terms of an initial contact size and reproduced the round vertical profiles. This method was applied to investigate the effects of a contact size, space in dense patterns, and process temperature on the flow amount. Also, the interface of PR flow simulation linking to lithography was set up and used to optimize the layout design to get the target contact sizes. As a result, the PR flow model integrated with lithography and etch models can be effectively used in analyzing defects considering the pre/post processes as well as predicting the contact patterning process and optimizing the layout.

REFERENCES

[1] Solid-C, SIGMA-C GmbH, 81737 Munchen, Germany.

[2] Prolith, FINLE Tech. Inc., Austin, Texas, USA.

[3] T. S. Cale, B. R. Rogers, T. P. Merchant, and L. J. Borucki, *J. Comp. Mat. Sci,* **12**, p333, 1998.

[4] Z.-K. Hsiau, E. C. Kan, J. P. McVittie, and R. W. Dutton, *IEEE Trans. Electron Devices,* **44,** p1375, 1997.

[5] W.-Y. Chung, J.-J. Oh, , T.-K. Kim, J.-K. Shin, K.-I. Seo, Y.-K. Park, and J.-T. Kong, *SISPAD*, p127, 2000.

[6] B.-K. Kim, S.-K. Lee, D.-Y. Lee, J.-W. Lee, and J.-L. Nam, *SPIE,* **4344**, p297, 2001.

[7] R. F. Probstein, "Physicochemical Hydrodynamics," Butterworths, Boston, 1989.

[8] R. B. Bird, W. E. Stewart, and E. N. Lightfoot, "Transport Phenomena," JohnWiley&Sons, New York, NY, p83, 1960.

[9] CFD-ACE+, CFD Research Corp., Huntsville, AL, USA.